Eco-Friendly Synthesis of Ag-ZnO Nanocomposite Using Aloe-Vera, Hibiscus Sabdariffa Plants and Their Antibacterial and Anti-fungi Activities

Noorullah Mohammed Nemma[1a*] and Zainab Sabeeh Sadeq[1b]
[1]*Department of Physics, College of Science, University of Baghdad, Baghdad, Iraq*
[b]E-mail: zainab.sadeq@sc.uobaghdad.edu.iq
[a*]Corresponding author: nourallah.mohammed1204a@sc.uobaghdad.edu.iq

Abstract

The current study used extracts from the aloe vera (AV) plant and the hibiscus sabdariffa flower to make Ag-ZnO nanoparticles (NPs) and Ag-ZnO nanocomposites (NCs). Ag/ZnO NCs were compared to Ag NPs and ZnO NPs. They exhibited unique properties against bacteria and fungi that aren't present in either of the individual parts. The Ag-ZnO NCs from AV showed the best performance against E. coli, with an inhibition zone of up to 27 mm, compared to the other samples. The maximum absorbance peaks were observed at 431 nm and 410 nm for Ag NPs, at 374 nm and 377 nm for ZnO NPs and at 384 nm and 391 nm for Ag-ZnO NCs using AV leaf extract and hibiscus sabdariffa flower extract, respectively. Using field emission-scanning electron microscopes (FE-SEM), the green synthesis of the shown NPs and NCs was found. The Ag NPs particle sizes ranged from 16.99 to 26.39 nm for AV and from 13.11 to 29.50 nm for hibiscus sabdariffa flowers, respectively. The particle size of ZnO NPs ranged from 23.04 to 32.58 nm and from 37.99 to 79.59 nm via AV and hibiscus sabdariffa flowers, respectively. Finally, the particle size of the Ag/ZnO nanocomposite ranged from 22.39–40.05 nm and from 59.73–87.05 nm via the AV and hibiscus sabdariffa flowers, respectively.

1. Introduction

In recent years, there has been significant global research focus on metal nanoparticles (NPs) and metal oxide semiconductor nanocomposites due to their remarkable optical, electrical, and chemical characteristics, as well as their promising range of potential applications [1-8]. Lately, there have been physical and chemical approaches used to synthesize Ag, ZnO, and Ag-ZnO nanomaterials [9-12]. However, a lot of these approaches need risky and harmful substances, high-cost items, and extraordinary lab conditions such as high heat and pressure, as well as longer processing times are required. As a result, there is always a need for a simplistic, environmentally safe approach for producing perfect-performance, cost-effective Ag, ZnO NPs and Ag-ZnO nanocomposite [13, 14]. Researchers have been focused on altering and coating semiconductor nanoparticles which include ZnO with metallic particles like Ag and Au, in order to develop nanocomposites [15-18].

Several studies have proved that metal/metal oxide nanoparticles and nanocomposites can be fabricated from plants, fungi, bacteria, as well as additional resources from nature. Therefore, choosing plants for nanocomposite synthesis may be preferable to other biological methods since it reduces the time-consuming procedures of maintaining cell cultures and has the potential to be scaled up to large-scale nanoparticle production [19-28]. All the parts of plants, such as flowers, fruits, leaves, stems, and roots can be used to create nanoparticles [29-35]. A new and intriguing approach to the development of these natural nano-factories has been provided by plants' capacity to produce metal nanoparticles. In comparison to microorganisms and

enzymes that require expensive production processes, plants have more advantages as sustainable and renewable resources since they can transform around 75% of the light energy from the sun into chemical energy [36, 37]. Moreover, plant extracts include capping agents for nanoparticle stability [38].

Furthermore, the interaction between Ag and ZnO in the Ag-ZnO NCPs can inhibit bacteria and fungi effectively [39, 40]. The anti-bacterial and antifungal activities of Ag-ZnO NCPs have been proven against gram-positive, Gram-negative bacteria and Candida [3, 41-45]. The present study, investigated the antibacterial activity of gram-positive, Gram-negative bacteria and the anti-fungi of Ag NPs, ZnO NPs and Ag-ZnO nanocomposite (synthesized from the extract of Aole vera gel and hibiscus sabdariffa flowers) using 2 g/m against gram-positive (S. aureus), Gram-negative (E. coli), (Kleb. Sp.) and Candida albicans fungi.

2. Experimental Work
2.1. Materials

The high purity chemicals such as zinc nitrate hexahydrate (Zn $(NO_3)_2 \cdot 6H_2O$), silver nitrate ($AgNO_3$), hydrochloric acid (HCL) and methyl red, were purchased from Allied, Carlo erba and Himedia chemical companies and used as received. The aloe vera (AV) plant and hibiscus sabdariffa leaves were purchased from local markets. The glassware was cleaned and washed twice with distilled water (DW) and ethanol and the items were dried for several hours in the oven before use.

2.2. Preparation of Ag NPs, ZnO NPs and Ag-ZnO Nanocomposites

Fig. 1 shows steps of preparation of the Ag NPs, ZnO NPs and Ag-ZnO nanocomposites. The first step started by extracting AV through washing, cutting and taking the gel only using a mixer. Then, 100 g of the gel was dissolved in 300 ml of DW using a magnetic stirrer for 30 min and left to be cooled and the resultant was centrifuged at 4000 rpm for about 10 min. Then, $AgNO_3$ solution was diluted to 0.1M using a magnetic stirrer at 60 °C for 30 min. On the other hand, a mass of 2.97 g of Zn $(NO_3)_2 \cdot 6H_2O$ was dissolved in 100 ml of DW to obtain 0.5 M concentration. Then, 200 ml of HCl was added dropwise to increase the temperature to 170 °C by vigorously stirring to fully melt and the solution color changed from white to transparent.

For Ag-ZnO nanocomposite, 100 ml of AV extract was divided equally into 50 ml added to 100 ml of $AgNO_3$ and 50 ml added to 100 ml of Zn $(NO_3)_2 \cdot 6H_2O$ and mixed carefully. Then, 100 ml of Ag NPs, which was prepared previously, was slowly added to 100 ml of ZnO NPs at 60 °C with continuous stirrer. A similar method was adopted to prepare Ag-ZnO nanocomposite via hibiscus sabdariffa flower by preparing the extract by washing it thoroughly with DW. After being dried under sunlight and grinded into small pieces, 2 g of Ag-ZnO was dissolved in 100 ml of DW using a magnetic stirrer at 60 °C for 30 min. The red extract was filtered twice with cotton wool balls, and 100 ml of aqueous extract was taken and the same procedure was repeated. Finally, all the solutions were deposited on slides by drop casting method for further experiments.

2.3. Antibacterial and Anti-Fungi Activities

The present work studied the effect of Ag NPs, ZnO NPs and Ag-ZnO nanocomposites (synthesized from the extract of AV leaves and hibiscus sabdariffa flowers prepared by green method) on two types of bacteria: gram-positive (S. aureus), Gram-negative (E. coli and Kleb. Sp). This was achieved by putting 2 g of a nanocomposite to each petri dish which contains bacteria. It was also studied the inhibition action as anti-fungal against Candida albicans using agar method with a

sterile plate, and an autoclave condition. A mass of 3.8 g of Mueller Hinton agar was diluted in 100 ml of DW and then added to the petri dish and kept in an incubator at 37°C for about 18–24 h [46-48]. Finally, the bacterial and fungal cultures with sterile swab were added to the petri dishes which were contained the medium. The inhibition zone diameters were measured in millimeters.
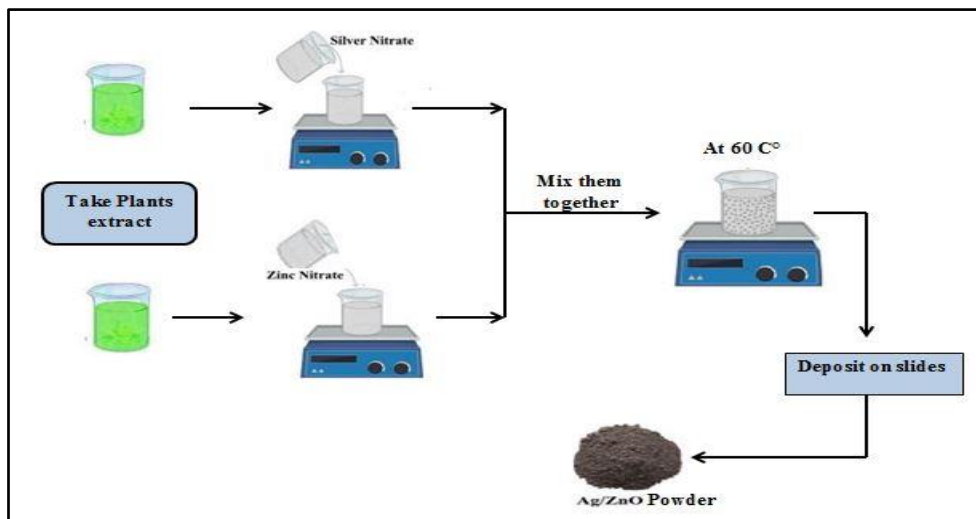

Figure 1: Preparation of Ag, ZnO NPs and Ag- ZnO nanocomposite method.

3. Characterization

The structural analysis of the samples was examined using X-ray diffraction (XRD) to ascertain their degree of crystallinity. The spectrograms were captured using X-ray diffractometer (Two Perkin Elmer) which employed Cu Kα radiation and covered a diffraction angle range of 20° to 80°. The morphological characteristics of the nanoparticles (NPs) were investigated through field-emission scanning electron microscopy (FE-SEM) (Inspect F-50 instrument, Holland). The elemental composition of the NPs was determined using energy-dispersive X-ray spectroscopy (EDX) (Thermo Fisher Scientific, USA), while the optical absorption spectra were measured using UV-visible absorption spectrometer (Lambda 365 Perkin Elmer).

4. Results and Discussion

4.1. FE-SEM and EDX Analyses

The morphology of the green synthesized Ag NPs, ZnO NPs and Ag-ZnO nanocomposites using AV and hibiscus sabdariffa extract respectively, were conducted by FE-SEM examination as shown in Fig. 2. The FE-SEM images showed the formation of agglomeration on the Ag-ZnO nanocomposite because the ZnO became a shell to the Ag NPs, while the aggregations were much less in the Ag NPs and ZnO NPs. Due to adding Ag to ZnO NPs, the morphology was varied and took many shapes such as spherical and nanorod. The results are in good agreement with the references [48, 49]. The particle size of Ag NPs was varied from 16.99 to 26.39 nm and from 13.11 to 29.50 nm, as shown in Fig. 2(a and b), respectively. The result is in agreement with N. Nemma and Z. Sadeq [50]. However, the particle size of ZnO NPs varied from 23.04 to 32.58 nm and from 37.99 to 79.59 nm as shown in Fig. 2(c and d), respectively. Finally, the particle size of Ag-ZnO nanocomposite ranged from 22.39 to 40.05 nm and from 59.73 to 87.05 nm shown in Fig. 2(e and f) via AV and hibiscus sabdariffa, respectively.

The EDX results demonstrated the Ag NPs, ZnO NPs and Ag-ZnO nanocomposite via both AV and hibiscus sabdariffa extracts. The synthesis exhibited a

distinct optical absorption band peak at approximately 3 keV. This characteristic absorption is commonly associated with metallic silver nanoparticles (Ag NPs) as shown in Fig. 3(a and b) due to surface plasmon resonance. The presence of oxygen signals in the EDX spectrum of the Ag NPs could be due to few different factors such as surface oxidation especially when it exposed to air or other oxidizing conditions, and sometimes, during sample preparation or handling. The EDX spectra in Fig. 3(c and d) showed the synthesis of ZnO NPs, whereas the spectra in Fig. 3(e and f) showed that Ag-ZnO nanocomposites which were synthesized in the presence of Ag and ZnO and with the impurities are associated with samples preparation procedures.

The presence of C, O, N, Ca, Mg, Si, Na and Cl were confirmed through EDX spectroscopy, and it is associated with the phenolic components of the extracts that adsorbed onto the nano-surface of the synthesized samples that remained during the process.
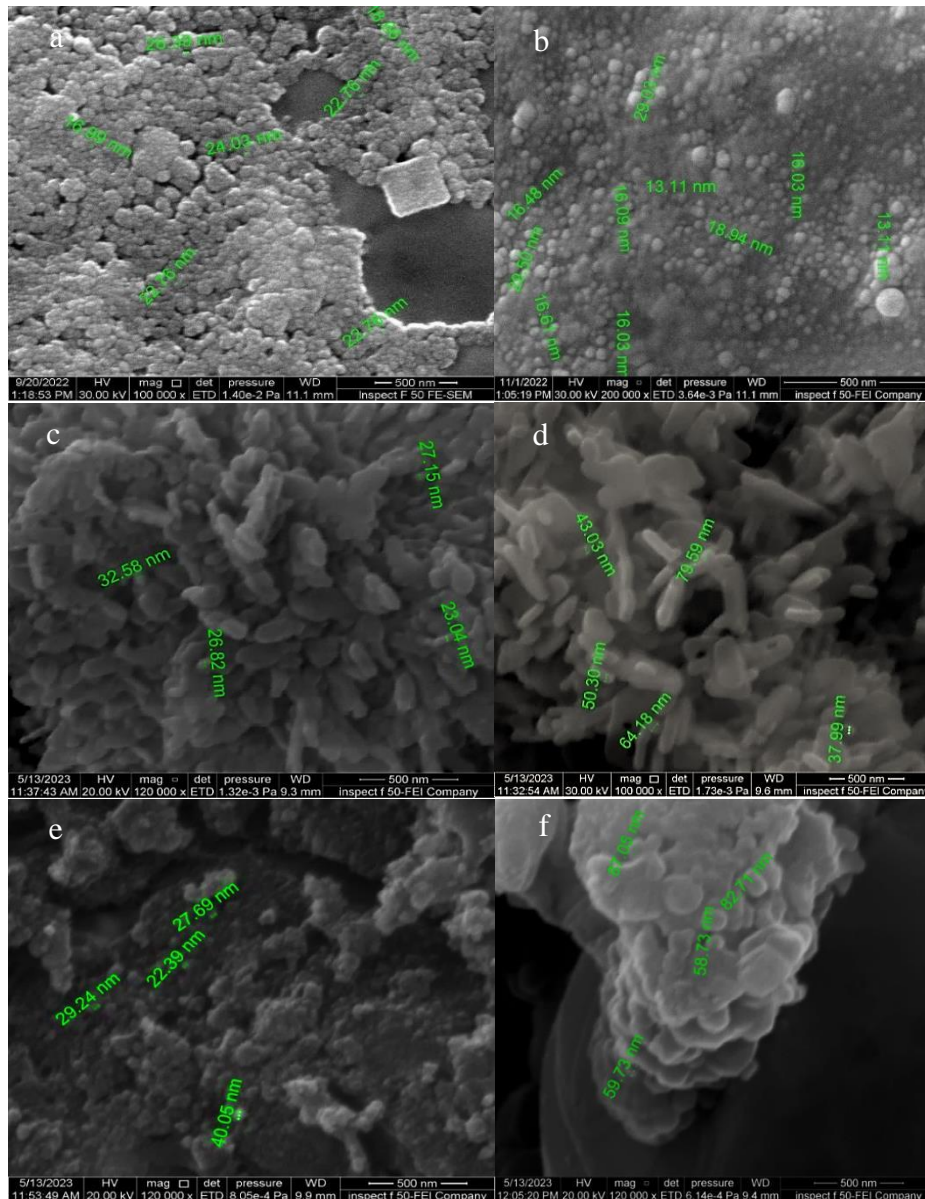

Figure 2: *FE-SEM images of: (a, b)Ag NPs formed via AV and hibiscus sabdariffa, (c, d) ZnO NPs formed via AV and hibiscus sabdariffa, (e, f) Ag/ZnO nanocomposite formed via AV and hibiscus sabdariffa.*

a

Element	Atomic %	Atomic % Error	Weight %	Weight % Error
C	28.4	0.3	11.9	0.1
N	12.4	0.5	6.1	0.2
O	40.2	0.8	22.4	0.5
Cl	4.6	0.1	5.7	0.1
Ag	14.4	0.1	54.0	0.4

b

Element	Atomic %	Atomic % Error	Weight %	Weight % Error
C	15.8	0.2	7.4	0.1
N	17.9	0.3	9.8	0.1
O	54.7	0.5	34.1	0.3
Ag	11.6	0.0	48.7	0.2

c

Element	Atomic %	Atomic % Error	Weight %	Weight % Error
C	30.3	0.6	17.1	0.3
N	5.4	0.6	3.5	0.4
O	38.6	0.4	29.0	0.3
Cl	20.3	0.1	33.8	0.1
Zn	5.4	0.0	16.6	0.1

d

Element	Atomic %	Atomic % Error	Weight %	Weight % Error
C	27.3	0.9	14.1	0.5
N	4.4	0.9	2.6	0.5
O	33.2	0.8	22.9	0.5
Mg	2.1	0.1	2.2	0.1
Cl	23.4	0.1	35.8	0.2
Ca	3.8	0.0	6.6	0.1
Zn	5.5	0.1	15.4	0.2

e

Element	Atomic %	Atomic % Error	Weight %	Weight % Error
C	19.9	0.3	8.1	0.1
N	8.5	0.7	4.5	0.4
O	27.6	0.7	15.0	0.4
Cl	9.8	0.1	11.2	0.1
Ca	2.0	0.0	3.0	0.1
Zn	6.8	0.1	27.3	0.2
Ag	7.7	0.1	31.5	0.4

f

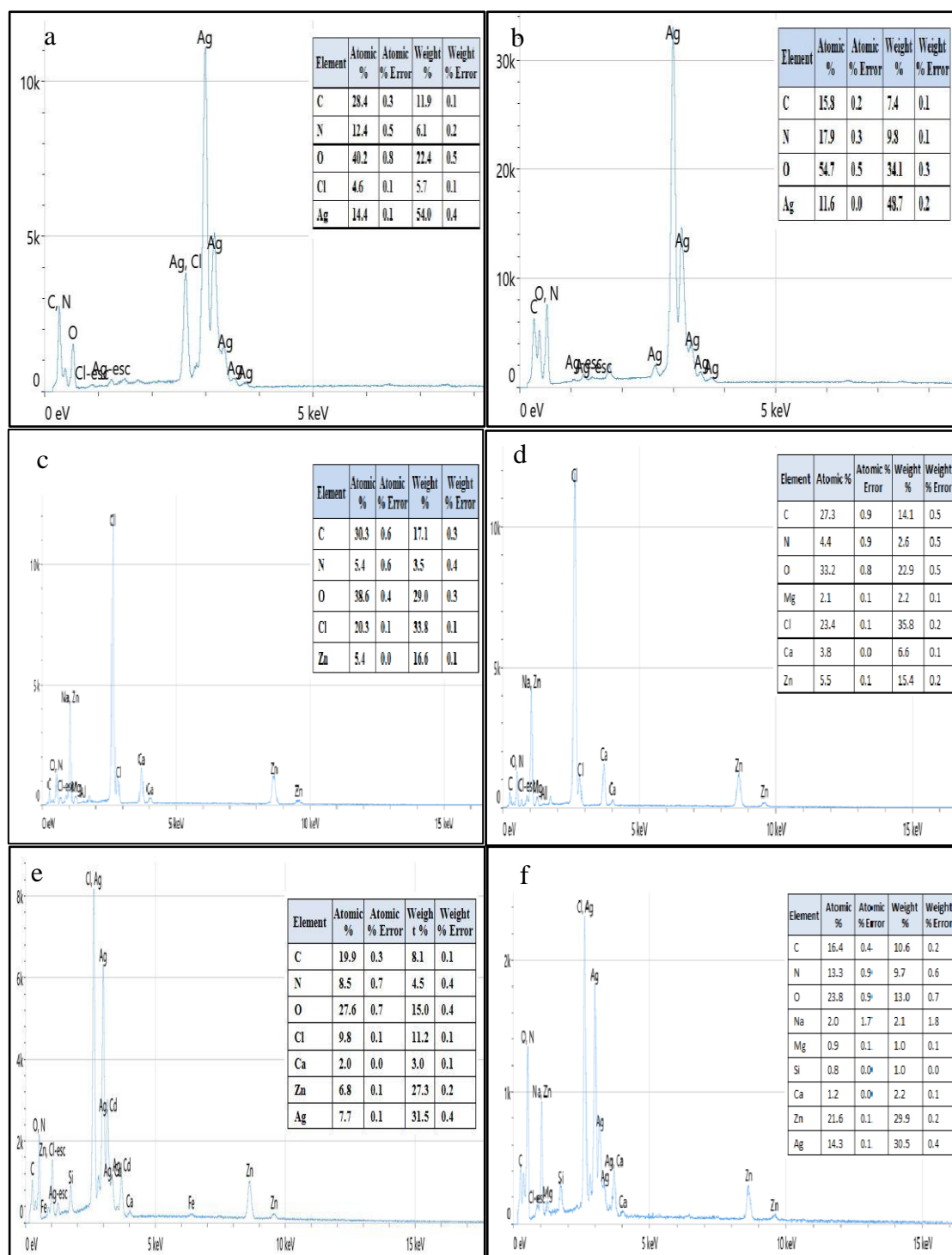| Element	Atomic %	Atomic % Error	Weight %	Weight % Error
C	16.4	0.4	10.6	0.2
N	13.3	0.9	9.7	0.6
O	23.8	0.9	13.0	0.7
Na	2.0	1.7	2.1	1.8
Mg	0.9	0.1	1.0	0.1
Si	0.8	0.0	1.0	0.0
Ca	1.2	0.0	2.2	0.1
Zn	21.6	0.1	29.9	0.2
Ag	14.3	0.1	30.5	0.4

Figure 3: EDX of (a and b) Ag NPs formed via AV and hibiscus sabdariffa (c and d) ZnO NPs formed via AV and hibiscus sabdariffa (e and f) Ag-ZnO nanocomposite formed via AV and hibiscus.

4.1. UV- visible Spectroscopy

The UV-visible spectrophotometer showed that the maximum absorbance of the synthesized Ag NPs was at 431 nm using AV leaf extract and at 410 nm using hibiscus sabdariffa flower extract, as shown in Fig. 4(a). The results agree with N. Nemma and Z. Sadeq [50]. Furthermore, a noticeable change in the color of the solution to gray was observed indicating the presence of surface plasmon resonance (SPR) of Ag NPs. While the absorbance of ZnO NPs displayed a maximum absorption peak at 374 and 377 nm using AV and hibiscus sabdariffa plant extracts,

respectively, as shown in Fig.4(b). On the other hand, the Ag-ZnO nanocomposite exhibited absorption peaks at 384 and 391 nm using AV and hibiscus sabdariffa extracts, respectively.
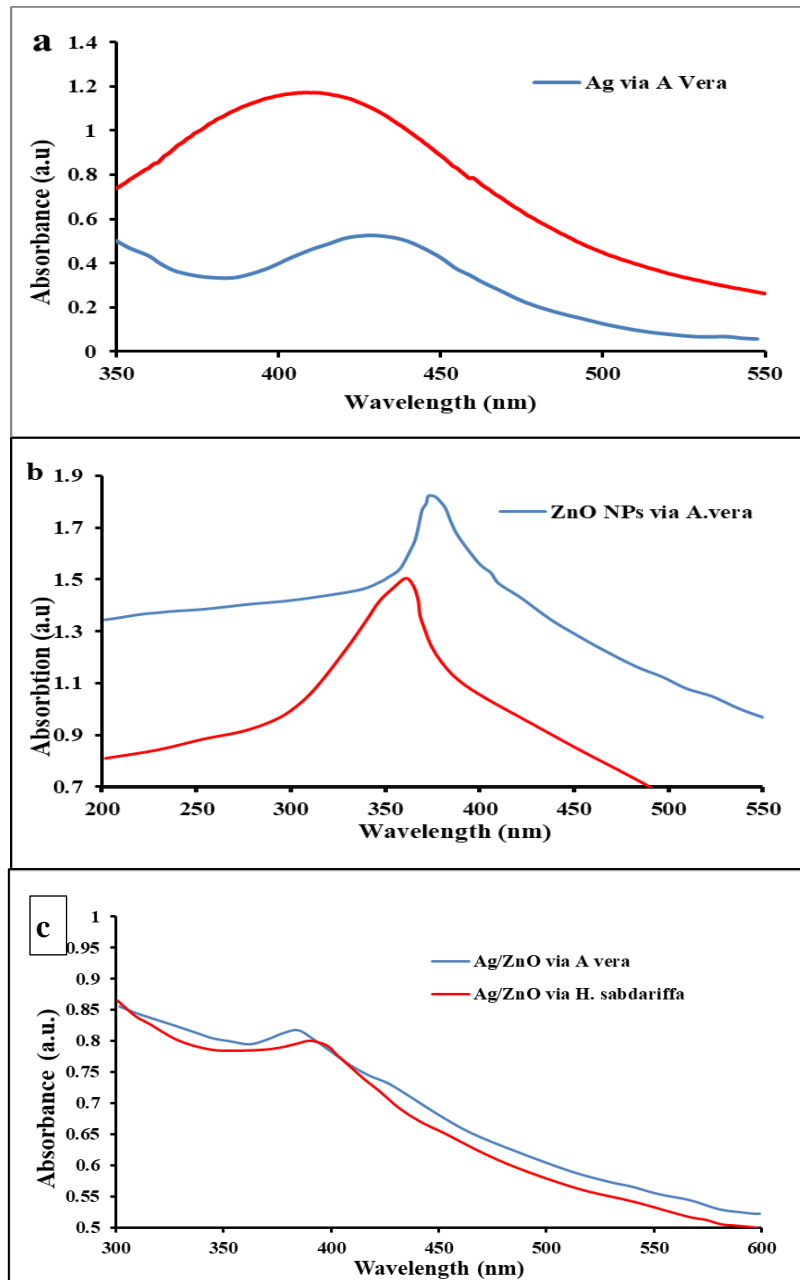

Figure 4: UV- Visible absorption of (a) Ag NPs, (b) ZnO NPs and (c) Ag-ZnO nanocomposite formed via AV and hibiscus sabdariffa.

4.2. Antibacterial and Anti-Fungi Studies

The inhibition zones were measured after 24 hrs as shown in Table 1, and was noticed that the Ag-ZnO nanocomposite which was prepared using AV plant extract was more effective as antibacterial and anti -fungi compared first with Ag/ZnO nanocomposite prepared using hibiscus sabdariffa flower extract, then compared with Ag NPs, ZnO NPs and the Ag NPs were the least efficient. From the results in the Table 1 and Fig. 5, the samples that prepared with AV plant extract have larger inhibition zones than the sample prepared with hibiscus sabdariffa flower extract. This mean that the AV plant extracts is more effective at inhibiting the growth of

bacteria and fungi than hibiscus sabdariffa flower extract. This could be due to the presence of certain compounds in the AV extract that are not present in the hibiscus sabdariffa extract, or because of using higher concentrations.

Table 1: The measured inhibitions zones.

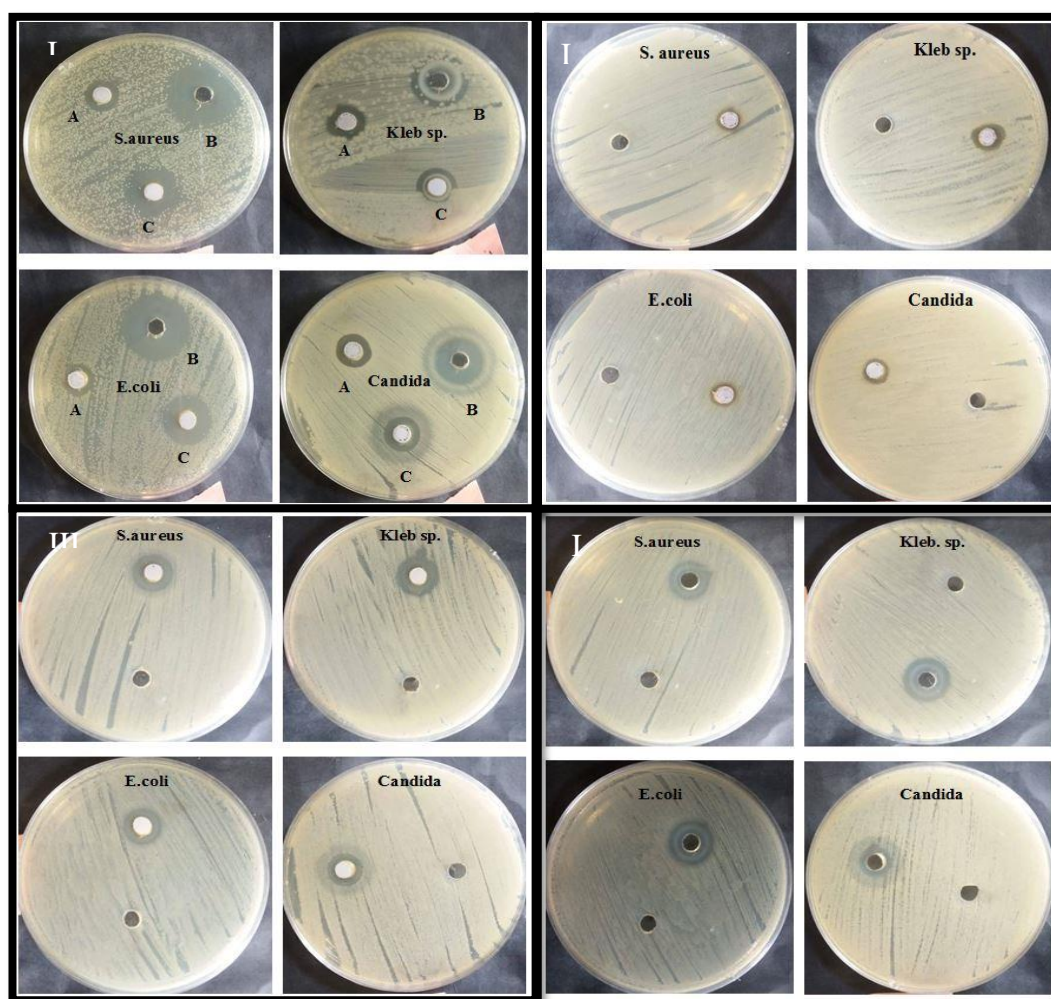| Bactria and fungal	Ag NPs		ZnO NPs		Ag/ZnO NPs	
Plant extract	AV	hibiscus sabdariffa	AV	hibiscus sabdariffa	AV	hibiscus sabdariffa
S. aureus	17	12	17	15	25	16
Kleb. Sp.	13	12	15	15	26	18
E. coli	13	12	18	15	27	18
Candida	14	13	14	13	20	15

Figure 5: The effect of (I) Ag NPs, ZnO NPs and Ag-ZnO nanocomposite formed via AV extract;(A) represents the Ag NPs effect, (B) the Ag/ZnO nanocomposite effect, and (C) the ZnO NPs effect. (II) Ag NPs formed via hibiscus sabdariffa extract, (III) ZnO NPs formed via hibiscus sabdariffa extract, (IV) Ag-ZnO nanocomposite formed via hibiscus sabdariffa extract.

5. Conclusions

In this study, Ag NPs, ZnO NPs and Ag-ZnO nanocomposite were fabricated using an easy, eco-friendly, and inexpensive green synthesis approach via AV and hibiscus sabdariffa plants extract in different ways. The XRD and EDX measurements

showed the presence of Ag and ZnO elements and confirmed their existence in the wurtzite hexagonal phase of the ZnO. The FE-SEM results indicated the prevalence of agglomerated NPs, with structures such as clustered NPs, spherical shapes, or rod-like nanostructures. The UV-visible spectra results demonstrated enhanced absorption in the visible light region compared to pure ZnO, indicating improved light absorption properties of the nanocomposite. This study suggests that the addition of ZnO to Ag leads to an increase the antibacterial and anti-fungal properties of the nanocomposites. However, Ag-ZnO nanocomposite, which was prepared with AV extract, showed higher antibacterial and anti-fungal activity with inhibition zones ranging from 20 to 27 mm compared to the same nanocomposite prepared using hibiscus sabdariffa flower extract, and also compared to Ag and ZnO NPs.

Acknowledgements

Conflict of Interest

Authors declare that they have no conflict of interest.

References

1. B. Baruwati and R. S. Varma, Chem. Sus. Chem.: Chem. Sust. Ener. Mat. **2**, 1041 (2009).
2. R. Sahay, V. J. Reddy, and S. Ramakrishna, Int. J. Mech. Mat. Eng. **9**, 1 (2014).
3. Z. S. Sadeq, Z. F. Mahdi, and A. M. Hamza, Mat. Lett. **254**, 120 (2019).
4. W. A. Sami and Z. S. Sadeq, in AIP Conference Proceedings (AIP Publishing, 2022). p.
5. Z. S. Sadeq, Iraqi J. Sci. **63**, 170 (2022).
6. R. C. Fierascu, A. Ortan, S. M. Avramescu, and I. Fierascu, Molecules **24**, 3418 (2019).
7. E. Da'na, A. Taha, and E. Afkar, Appl. Sci. **8**, 1922 (2018).
8. A. Lalitha, R. Subbaiya, and P. Ponmurugan, Int. J. Curr. Microbiol. App. Sci. **2**, 228 (2013).
9. M. N. Nadagouda and R. S. Varma, Green Chem. **10**, 859 (2008).
10. N. D. S. Zambri, N. I. Taib, F. Abdul Latif, and Z. Mohamed, Molecules **24**, 3803 (2019).
11. M. Zare, K. Namratha, S. Alghamdi, Y. H. E. Mohammad, A. Hezam, M. Zare, Q. A. Drmosh, K. Byrappa, B. N. Chandrashekar, and S. Ramakrishna, Sci. Repor. **9**, 8303 (2019).
12. A. Verma and M. S. Mehata, J. Radiat. Res. App. Sci. **9**, 109 (2016).
13. C. Karunakaran, V. Rajeswari, and P. Gomathisankar, Sol. Stat. Sci. **13**, 923 (2011).
14. I. Matai, A. Sachdev, P. Dubey, S. U. Kumar, B. Bhushan, and P. Gopinath, Coll. Sur. B: Biointer. **115**, 359 (2014).
15. S. G. Gnanamani and V. T. Mary, Indian J. Chem. Tech. **29**, 766 (2022).
16. B. A. Fahimmunisha, R. Ishwarya, M. S. Alsalhi, S. Devanesan, M. Govindarajan, and B. Vaseeharan, J. Drug Deliv. Sci. Tech. **55**, 101465 (2020).
17. T. P. Kumar, T. R. Mandlimath, P. Sangeetha, P. Sakthivel, S. Revathi, S. A. Kumar, and S. K. Sahoo, RSC Advan. **5**, 108034 (2015).

18. P. Luque, C. Soto-Robles, O. Nava, C. Gomez-Gutierrez, A. Castro-Beltran, H. Garrafa-Galvez, A. Vilchis-Nestor, and A. Olivas, J. Mat. Sci.: Mat. Elec. **29**, 9764 (2018).
19. J. Y. Song, H.-K. Jang, and B. S. Kim, Proc. Biochem. **44**, 1133 (2009).
20. A. Gallo, C. Bianco, T. Tosco, A. Tiraferri, and R. Sethi, J. Clean. Produc. **211**, 1367 (2019).
21. J. Huang, Q. Li, D. Sun, Y. Lu, Y. Su, X. Yang, H. Wang, Y. Wang, W. Shao, and N. He, Nanotechnology **18**, 105104 (2007).
22. R. S. Varma, Curr. Opin. Chem. Eng. **1**, 123 (2012).
23. M. N. Nadagouda, N. Iyanna, J. Lalley, C. Han, D. D. Dionysiou, and R. S. Varma, ACS Sus. Chem. Eng. **2**, 1717 (2014).
24. C. Karthik and K. Radha, Orient. J. Chem. **32**, 735 (2016).
25. S. Acevedo, J. Arevalo-Fester, L. Galicia, R. Atencio, E. Plaza, and E. Gonzalez, J. Nanomed. Res. **1**, 00009 (2014).
26. G. Franci, A. Falanga, S. Galdiero, L. Palomba, M. Rai, G. Morelli, and M. Galdiero, Molecules **20**, 8856 (2015).
27. P. Roy, B. Das, A. Mohanty, and S. Mohapatra, App. Nanosci. **7**, 843 (2017).
28. H. Djahaniani, M. Rahimi-Nasrabadi, M. Saiedpour, S. Nazarian, M. Ganjali, and H. Batooli, Int. J. Food Proper. **20**, 922 (2017).
29. T. Sinha, M. Ahmaruzzaman, P. P. Adhikari, and R. Bora, ACS Sus. Chem. Eng. **5**, 4645 (2017).
30. D. Hebbalalu, J. Lalley, M. N. Nadagouda, and R. S. Varma, ACS Sus. Chem. Eng. **1**, 703 (2013).
31. A. Lagashetty and S. K. Ganiger, Heliyon **5**, e02794 (2019).
32. M. Yadi, E. Mostafavi, B. Saleh, S. Davaran, I. Aliyeva, R. Khalilov, M. Nikzamir, N. Nikzamir, A. Akbarzadeh, Y. Panahi, and M. Milani, Artif Cells Nano. Biotech. **46**, S336 (2018).
33. D. Gnanasangeetha and S. D. Thambavani, Int. J. Pharm. Sci. Res. **5**, 2866 (2014).
34. S. Priyadarshini, S. Sulava, R. Bhol, and S. Jena, Cur. Sci. **117**, 1300 (2019).
35. A. Singh and M. Kaushik, Resul. Phys. **13**, 102168 (2019).
36. J. Kou and R. S. Varma, Chem. Sus. Chem. **5**, 2435 (2012).
37. B. Shan, Y. Z. Cai, M. Sun, and H. Corke, J. Agricult. Food Chem. **53**, 7749 (2005).
38. J. Rakaa, Baghdad Sci. J. **17**, 0670 (2020).
39. Y. Li, C. Gao, R. Long, and Y. Xiong, Mat. Today Chem. **11**, 197 (2019).
40. M. S. S. Danish, L. L. Estrella, I. M. A. Alemaida, A. Lisin, N. Moiseev, M. Ahmadi, M. Nazari, M. Wali, H. Zaheb, and T. Senjyu, Metals **11**, 80 (2021).
41. M. Hafeez, M. Zeb, A. Khan, B. Akram, Z. U. Abdin, S. Haq, M. Zaheer, and S. Ali, Micro. Res. Tech. **84**, 480 (2021).
42. R. K Sali, M. S Pujar, S. Patil, and A. H Sidarai, Advan. Mat. Lett. **12**, 1 (2021).
43. J. D. O. Primo, D. F. Horsth, J. D. S. Correa, A. Das, C. Bittencourt, P. Umek, A. G. Buzanich, M. Radtke, K. V. Yusenko, and C. Zanette, Nanomaterials **12**, 1764 (2022).
44. F. A. Alharthi, A. A. Alghamdi, N. Al-Zaqri, H. S. Alanazi, A. A. Alsyahi, A. E. Marghany, and N. Ahmad, Sci. Rep. **10**, 20229 (2020).
45. D. K. Patel, K. Patel, and S. Dhanabal, J. Acute Disease **1**, 47 (2012).
46. N. Khatoon, J. A. Mazumder, and M. Sardar, J. Nanosci. Curr. Res. **2**, 1000107 (2017).
47. S. Abbas, K. Hussain, Z. Hussain, R. Ali, and T. Abbas, Pharm. Anal. Acta. **7**, 522 (2016).

48. A. Barnasas, M. V. Karavasilis, C. Aggelopoulos, C. D. Tsakiroglou, and P. Poulopoulos, in Journal of Nano Research (Trans. Tech. Publ., 2020). p. 75.

49. J. Iqbal, N. Safdar, T. Jan, M. Ismail, S. Hussain, A. Mahmood, S. Shahzad, and Q. Mansoor, J. Mat. Sci. Tech. **31**, 300 (2015).

50. N. M. Nemma and Z. S. Sadeq, Chem. Meth. **7**, 325 (2023).

طريقه صديقة للبيئة لتخليق الجسيمات النانويةً Ag /ZnO باستخدام كلا من نبات الاولفيرا والكوجرات وتطبيقاتها ضد البكتريا والفطريات

نورالله محمد نعمة[1] و زينب صبيح صادق[1]

[1] قسم الفيزياء، كلية العلوم، جامعة بغداد، بغداد، العراق

الخلاصة

استخدمت الدراسة الحالية مقتطفات من نبات الصبار (AV) وزهرة الكركديه لصنع جزيئات Ag-ZnO النانوية (NPs) ومركبات Ag-ZnO النانوية وتمت مقارنة Ag/ZnO NCs مع Ag NPs و ZnO NPs ولقد أظهروا خصائص فريدة ضد البكتيريا والفطريات غير الموجودة في أي من الأجزاء الفردية. أظهرت Ag-ZnO NCs من AV أفضل أداء ضد E. coli ، مع منطقة تثبيط تصل إلى 27 ملم، مقارنة بالعينات الأخرى. وقد لوحظت قمم الامتصاص القصوى عند 431 نانومتر و410 نانومتر لـ Ag NPs ، عند 374 نانومتر و377 نانومتر لـ ZnO NPs وعند 384 نانومتر و391 نانومتر لـ Ag-ZnO NCs باستخدام مستخلص أوراق AV ومستخلص زهرة الكركديهsabdariffa ، على التوالي. باستخدام المجاهر الإلكترونية لمسح الانبعاثات الميدانية(FE-SEM) ، تم العثور على التوليف الأخضر لـ NPs و NCsالمبينة. تراوحت أحجام جسيمات Ag NPs من 16.99 إلى 26.39 نانومتر لـ AV ومن 13.11 إلى 29.50 نانومتر لزهور الكركديهsabdariffa ، على التوالي. تراوح حجم جسيمات ZnO NPs من 23.04 إلى 32.58 نانومتر ومن 37.99 إلى 79.59 نانومتر عبر زهور AV وزهور الكركديه sabdariffa ، على التوالي. أخيرًا، تراوح حجم الجسيمات للمركب النانوي Ag/ZnO من 22.39 إلى 40.05 نانومتر ومن 59.73 إلى 87.05 نانومتر عبر زهور AV وزهور الكركديهsabdariffa ، على التوالي.

الكلمات المفتاحيه: الطريقة الخضراء، نانو فضه، نانو زنك، خلطة نانو فضة ونانو زنك، مضاد للبكتريا والفطريات.